

Experimental status of the muon $g-2$ (and prospects for CLFV measurements)

Dinko Počanić, (for the Muon $g-2$ Collaboration)

University of Virginia

BEAUTY
2019

18th Int'l. Conf. on B-physics
BEAUTY 2019
Ljubljana, Slovenia
30 Sep. – 4 Oct. 2019



Lepton magnetic dipole moments

We recall g , the g -factor (or dimensionless gyromagnetic ratio):

$$\vec{\mu} = g \frac{e}{2m} \vec{S}.$$

- ▶ Dirac theory gives $g \equiv 2$ for a point particle.
- ▶ Quantum fluctuations give rise to the **anomalous magnetic moments**:

$$a = \frac{g - 2}{2} \neq 0.$$

Lepton magnetic dipole moments

We recall g , the g -factor (or dimensionless gyromagnetic ratio):

$$\vec{\mu} = g \frac{e}{2m} \vec{S}.$$

- ▶ Dirac theory gives $g \equiv 2$ for a point particle.
- ▶ Quantum fluctuations give rise to the **anomalous magnetic moments**:

$$a = \frac{g - 2}{2} \neq 0.$$

E.g., **electron anomaly** is extremely well reproduced by QED:

$$\left. \begin{aligned} a_e &= 0.001\,159\,652\,181\,61\,(23) \text{ [SM, } (\alpha/\pi)^5 \text{ order]}^* \\ a_e &= 0.001\,159\,652\,181\,28\,(18) \text{ [experiment, 0.15 ppb]}^\dagger \end{aligned} \right\} \text{ agreement: } \sim 1.1\sigma$$

insensitive to massive particle loops ($\Rightarrow a_e$ provides an alternative measurement of α_{em})

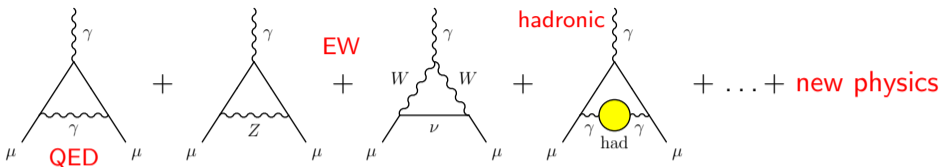
But, a_μ is much more sensitive than a_e to massive loops as: $(m_\mu/m_e)^2 \approx 43,000$.

* Aoyama, Kinoshita & Nio, *Atoms* **7** (2019) 1.

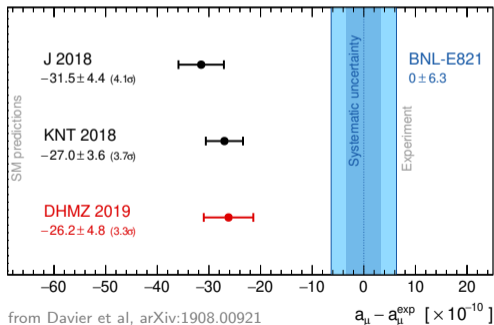
† Mohr et al., CODATA 2018, posted online 20 May 2019, to be published.

Muon anomalous magnetic moment (status mid-2019)

LO diagrams:



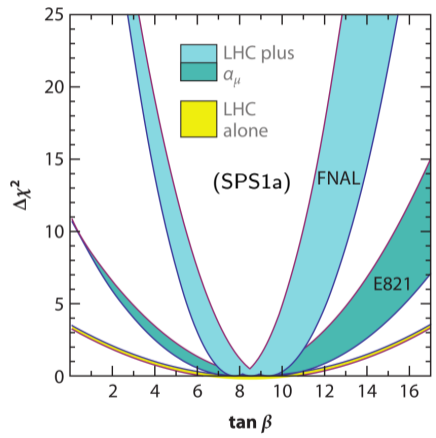
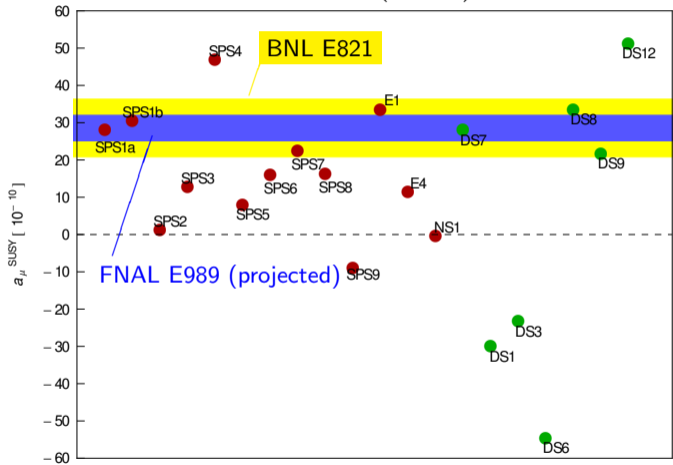
Term	Value ($\times 10^{-11}$)
QED ($\gamma + \ell$)*	$116\,584\,718.95 \pm 0.08$
HVP(lo) [Davier et al 19]	$6\,939 \pm 40$
HVP(nlo) [Davier et al 19]	-98.7 ± 0.9
HVP(nnlo) [Kurz et al 14]	12.4 ± 0.1
HLbL [Prades et al 09]	105 ± 26
EW [Gnendinger et al 13]	154 ± 1
Total SM [Davier et al 19]	$116\,591\,829 \pm 49_{\text{tot}}$



* Kinoshita et al 04-12, Kurz et al 16, Kataev 06, Passera 05

Example of new physics reach of a_μ : Supersymmetry

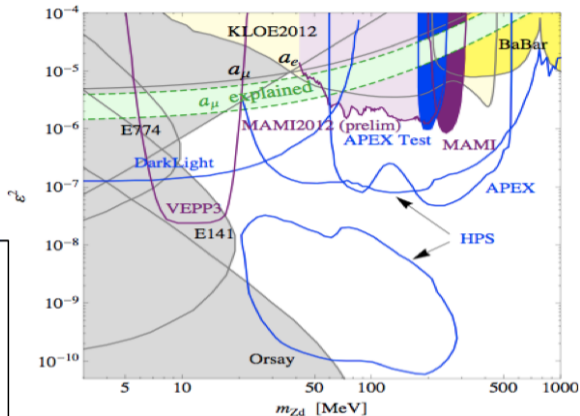
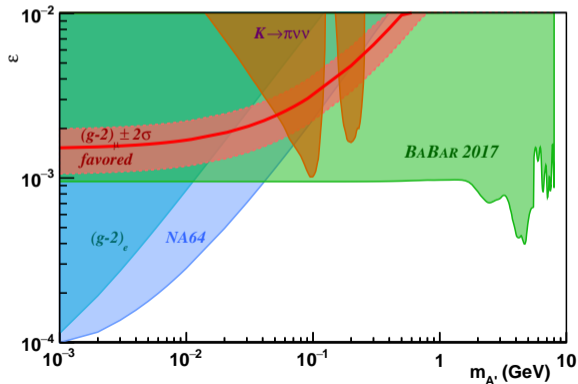
$a_\mu^{\text{SUSY}} \approx 13 \times 10^{-10} \tan \beta \operatorname{sgn}(\mu) \left(\frac{100 \text{ GeV}}{M_{\text{SUSY}}} \right)$, w. $\tan \beta = \frac{v_2}{v_1}$ (or $\frac{v_u}{v_d}$); μ is the strength of $\hat{H}_1 \hat{H}_2$ term ...



SUSY contributions to a_μ for select parameter sets [after C. Adam et al., EPJ C 171 (2011) 1520, and M. Alexander et al., arXiv:0802.3672].

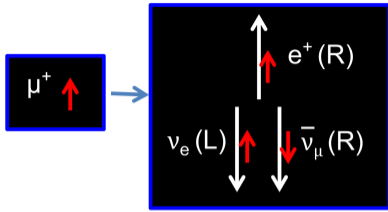
Dark photons:

status circa 2012 →



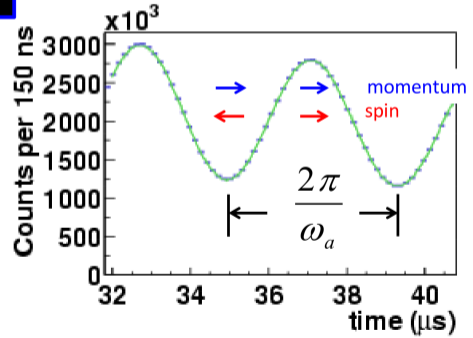
← 2017 BaBar results

Experiment: use properties of $\mu^+ \rightarrow e^+ \nu_e \bar{\nu}_\mu$ decay



Positron direction follows muon spin

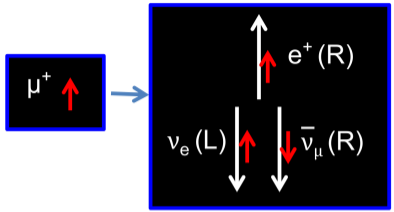
Highest energy positrons occur when muon spin and momentum are aligned (decay is boosted)



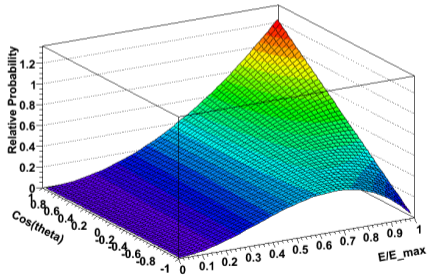
high energy positrons versus time

courtesy D. Hertzog

Experiment: use properties of $\mu^+ \rightarrow e^+ \nu_e \bar{\nu}_\mu$ decay

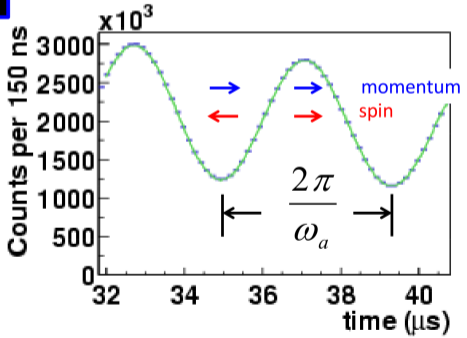


Positron direction follows muon spin



$$\theta = \angle(\vec{p}_e, \vec{p}_\mu)$$

courtesy D. Hertzog



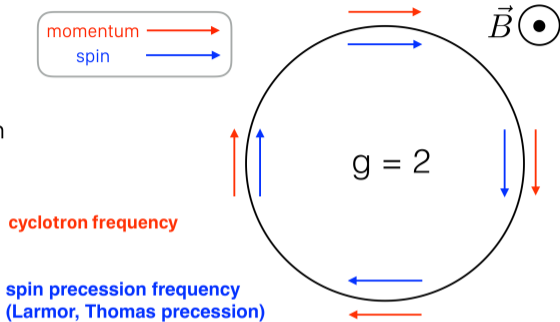
high energy positrons versus time

Measuring ω_a through correlation with p_μ

- Inject polarized muon beam (from pion decay) into ring
- Measure **difference** between spin precession and cyclotron frequencies

$$\vec{\omega}_C = -\frac{e}{\gamma m} \vec{B}$$

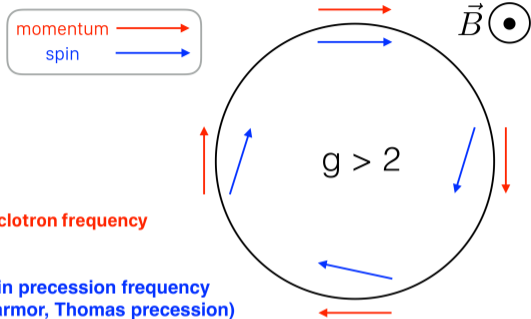
$$\vec{\omega}_S = -\frac{e}{\gamma m} \vec{B}$$



- If $g = 2$, difference of spin precession and cyclotron frequencies is zero

Measuring ω_a through correlation with p_μ

- Inject polarized muon beam (from pion decay) into ring
- Measure **difference** between spin precession and cyclotron frequencies



$$\vec{\omega}_C = -\frac{e}{\gamma m} \vec{B}$$

cyclotron frequency

$$\vec{\omega}_S = -\frac{e}{\gamma m} \vec{B} (1 + \gamma a_\mu)$$

spin precession frequency (Larmor, Thomas precession)

0 for $\gamma = 29.3$ ($p = 3.1$ GeV)

$$\vec{\omega}_a \equiv \vec{\omega}_S - \vec{\omega}_C = -\frac{e}{m} \left[a_\mu \vec{B} - \left(a_\mu - \frac{1}{\gamma^2 - 1} \right) \frac{\vec{\beta} \times \vec{E}}{c} \right]$$

E-field vertical focusing allowed at $p = 3.1$ GeV (higher-order a_μ contribution cancelled)

courtesy D. Flay

Muon $g - 2$: experimental status

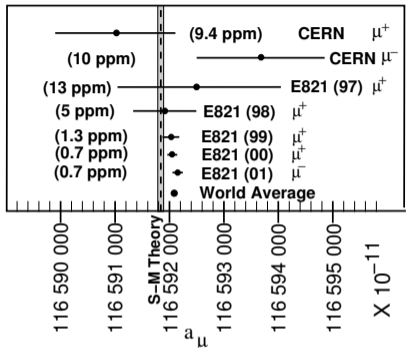
Dominated by results of BNL E821:

$$a_{\mu}^{\text{exp}} = 116\,592\,089\,(54)_{\text{stat}}\,(33)_{\text{syst}} \times 10^{-11}, \text{ or}$$

$$a_{\mu}^{\text{exp}} = 116\,592\,089\,(63)_{\text{tot}} \times 10^{-11}, \text{ i.e., a}$$

0.54 ppm result : statistical uncertainty dominates.

How to improve this result?

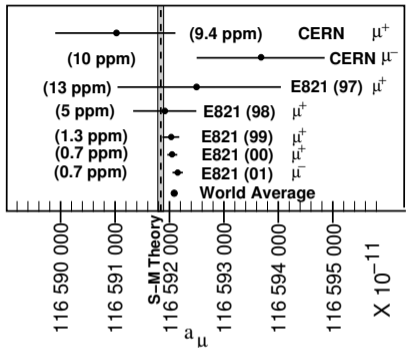


Dominated by results of BNL E821:

$$a_{\mu}^{\text{exp}} = 116\,592\,089 (54)_{\text{stat}} (33)_{\text{syst}} \times 10^{-11}, \text{ or}$$

$$a_{\mu}^{\text{exp}} = 116\,592\,089 (63)_{\text{tot}} \times 10^{-11}, \text{ i.e., a}$$

0.54 ppm result : statistical uncertainty dominates.



How to improve this result?

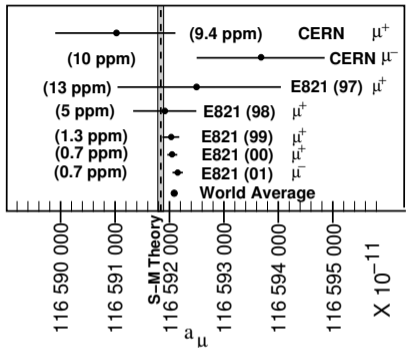
- ▶ Use a more intense beam at Fermilab: $21 \times$ statistics of BNL E821,
- ▶ improve a number of contributing systematics factors.

Dominated by results of BNL E821:

$$a_{\mu}^{\text{exp}} = 116\,592\,089\,(54)_{\text{stat}}\,(33)_{\text{syst}} \times 10^{-11}, \text{ or}$$

$$a_{\mu}^{\text{exp}} = 116\,592\,089\,(63)_{\text{tot}} \times 10^{-11}, \text{ i.e., a}$$

0.54 ppm result : statistical uncertainty dominates.



How to improve this result?

- ▶ Use a more intense beam at Fermilab: $21 \times$ statistics of BNL E821,
- ▶ improve a number of contributing systematics factors.

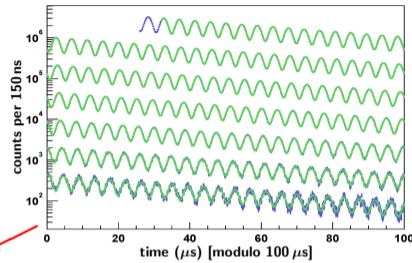
Goal for Fermilab E989:

- ▶ obtain overall $4 \times$ reduction in uncertainty, i.e., 0.14 ppm (total).



Determining a_μ

Rewriting B in terms of free proton precession frequency ω_p :



$$a_\mu = \frac{g_e \mu_p m_\mu \omega_a}{2 \mu_e m_e \langle \omega_p \rangle}$$

↖ ω_a \swarrow $\langle \omega_p \rangle$

From 2018 CODATA (Mohr et al., May 2019):

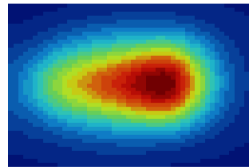
$g_e = -2.002\,319\,304\,362\,56\,(35)$ [0.17 ppt] [$(g-2)_e$, QED]

$\mu_p/\mu_e = -0.001\,519\,270\,377\,10\,(46)$ [0.3 ppb] [H maser]

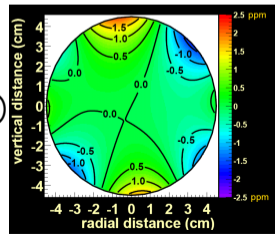
$m_\mu/m_e = 206.768\,2830\,(46)$ [22 ppb] [muonium HFS]

MuSEUM/J-PARC

Recall: E989 goal is **140 ppb** overall!



beam profile in μ SR

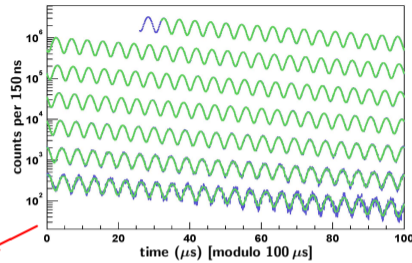




Determining a_μ

Rewriting B in terms of free proton precession frequency ω_p :

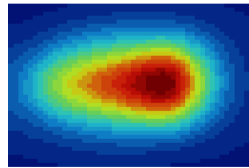
Two independent measurements required!



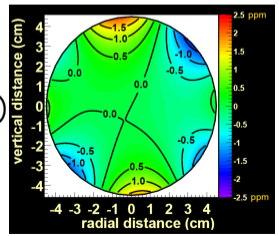
$$a_\mu = \frac{g_e \mu_p m_\mu \omega_a}{2 \mu_e m_e \langle \omega_p \rangle}$$

From 2018 CODATA (Mohr et al., May 2019):
 $g_e = -2.002\,319\,304\,362\,56(35)$ [0.17 ppt] [($g-2$) $_e$, QED]
 $\mu_p/\mu_e = -0.001\,519\,270\,377\,10(46)$ [0.3 ppb] [H maser]
 $m_\mu/m_e = 206.768\,2830(46)$ [22 ppb] [muonium HFS]
MuSEUM/J-PARC

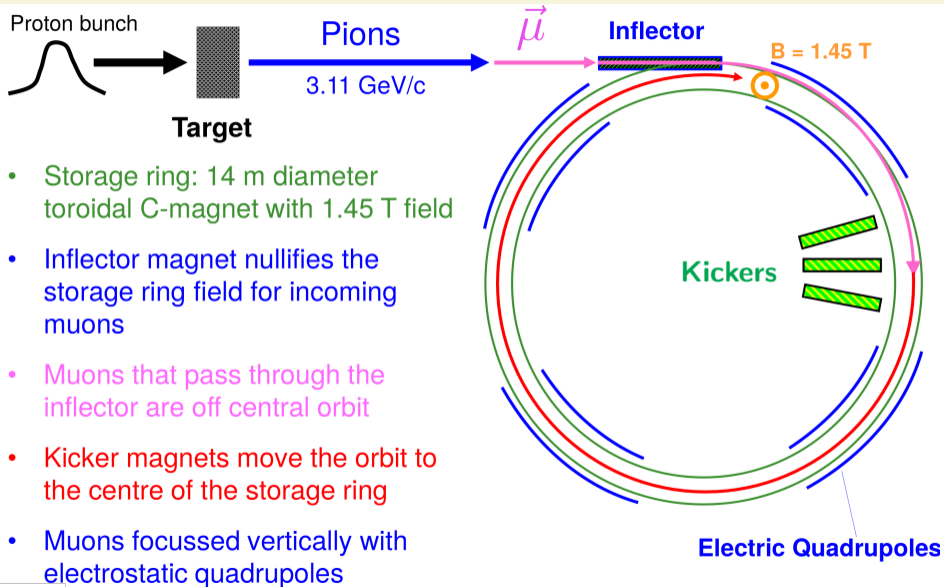
Recall: E989 goal is **140 ppb** overall!



beam profile in μ SR



Muon beam and storage



- Storage ring: 14 m diameter toroidal C-magnet with 1.45 T field
- Inflector magnet nullifies the storage ring field for incoming muons
- Muons that pass through the inflector are off central orbit
- Kicker magnets move the orbit to the centre of the storage ring
- Muons focussed vertically with electrostatic quadrupoles

B = 1.4513 T (~5200 A)

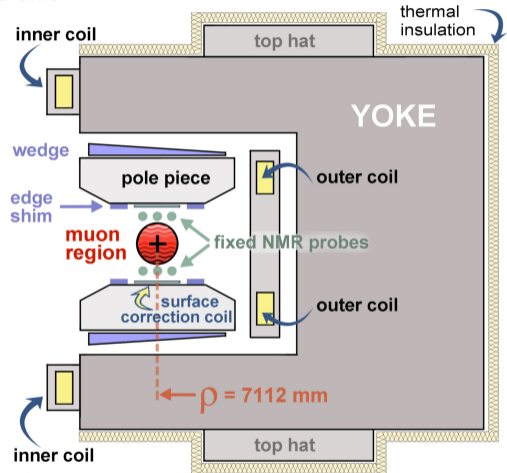
- Non-persistent current: fine-tuning of field in real time

12 C-shaped yokes

- 3 poles per yoke
- 72 total poles

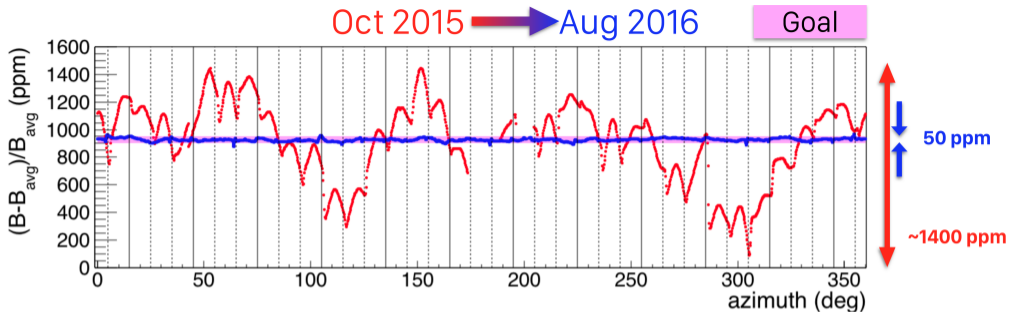
Shimming knobs

- Poles: shape field
- Top hats (30 deg, dipole)
- Wedges (10 deg, dipole, quadrupole)
- Edge shims (360 deg, quadrupole, sextupole)
- Laminations (360 deg, dipole, quadrupole, sextupole)
- Surface coils (360 deg, quadrupole, sextupole,...)

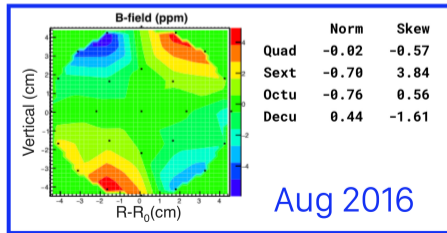
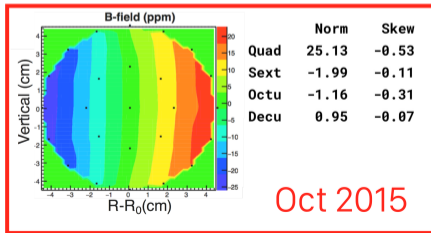


g-2 Magnet in Cross Section

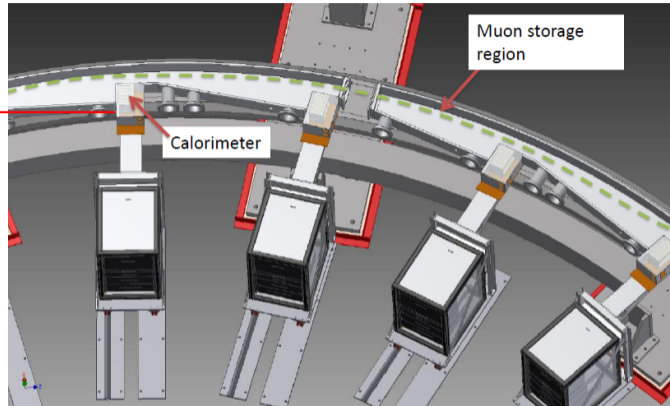
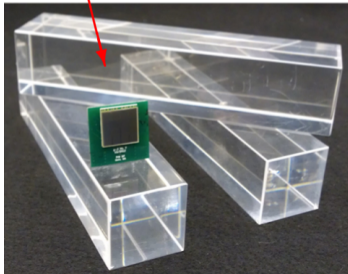
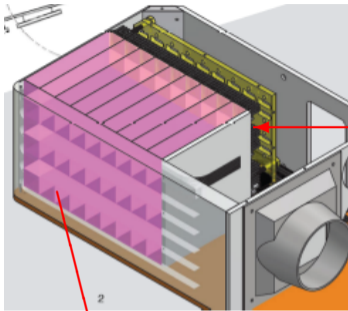
Shimming
results:



Azimuthally-Averaged Map

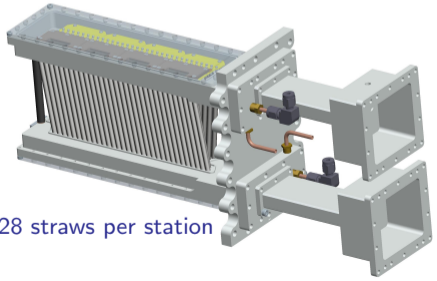
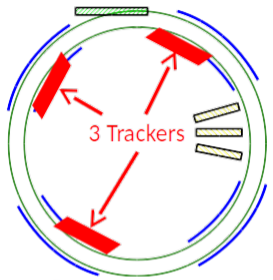


Calorimeters (ω_a measurement)

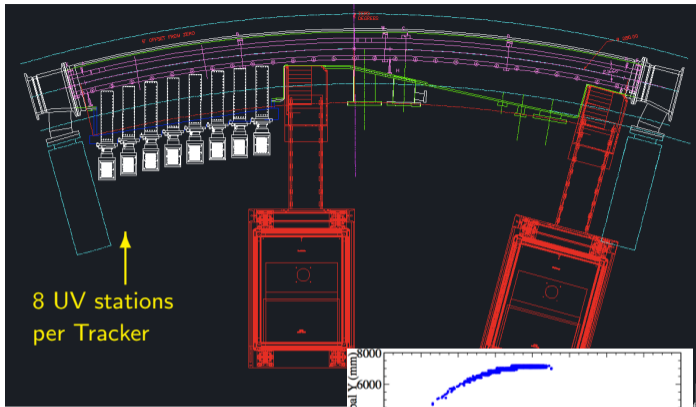


Individual positrons from muon decays are detected in 24 calorimeters; E and t extracted from waveforms. Each calo. segmented into 6×9 channels: Each PbF_2 crystal is read out by a Geiger-mode avalanche photodiode (SiPM).

Straw tube Trackers

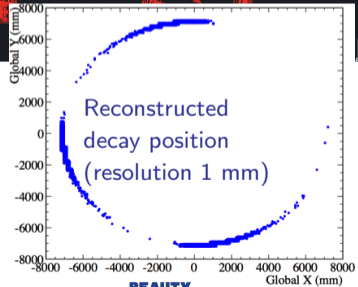


128 straws per station

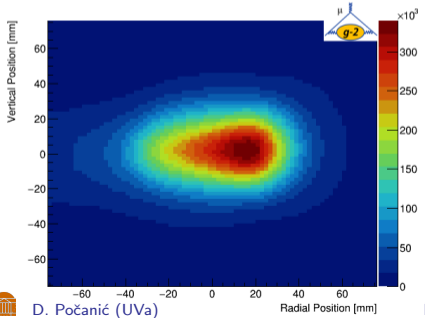
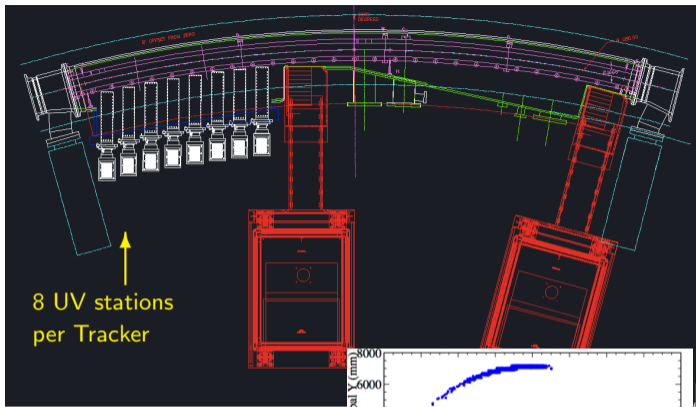
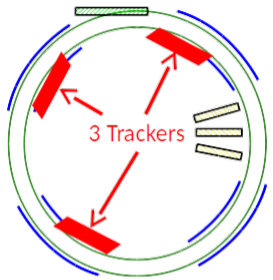


8 UV stations per Tracker

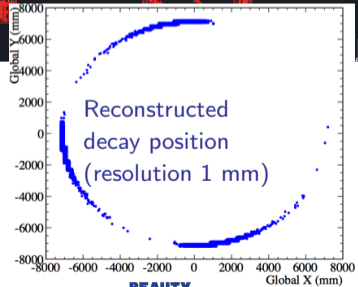
New for Fermilab E989 (did not exist in BNL E821); provide critical beam phase space and dynamics data.



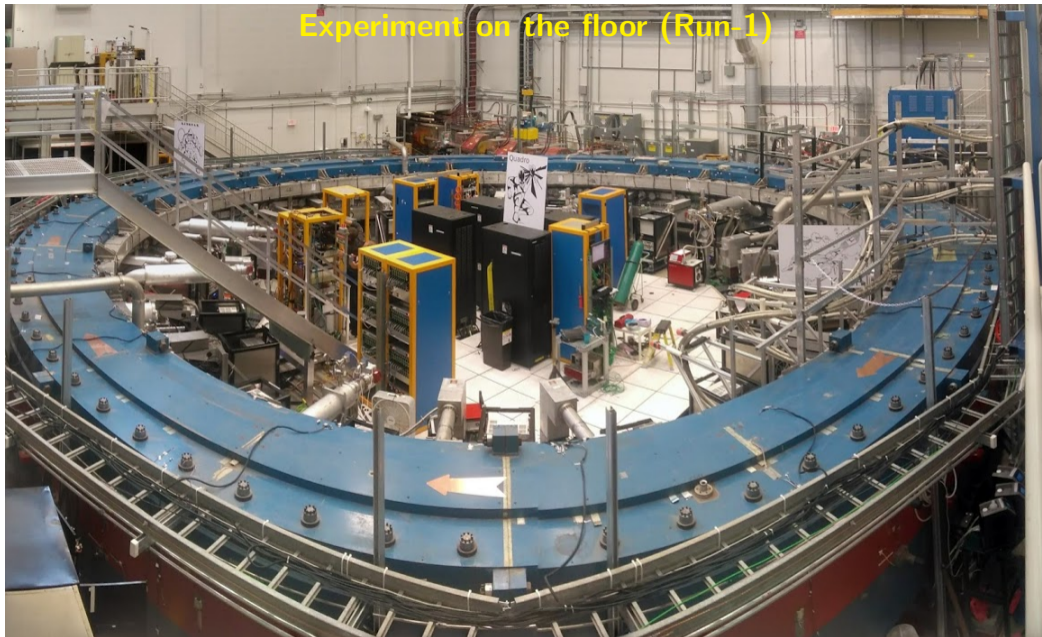
Straw tube Trackers



New for Fermilab E989
(did not exist in BNL E821);
provide critical beam phase
space and dynamics data.



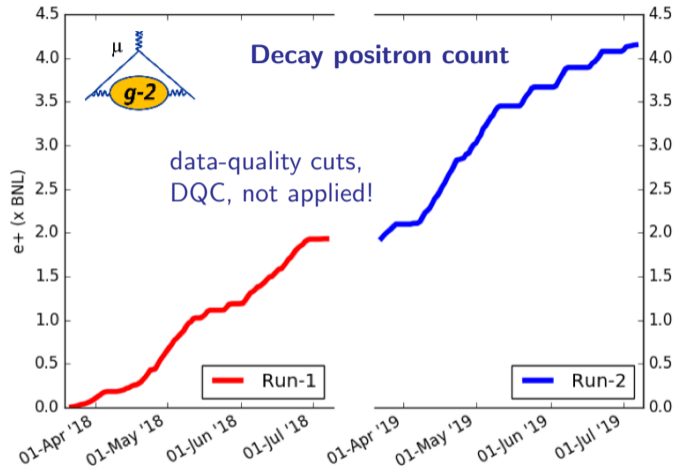
Experiment on the floor (Run-1)





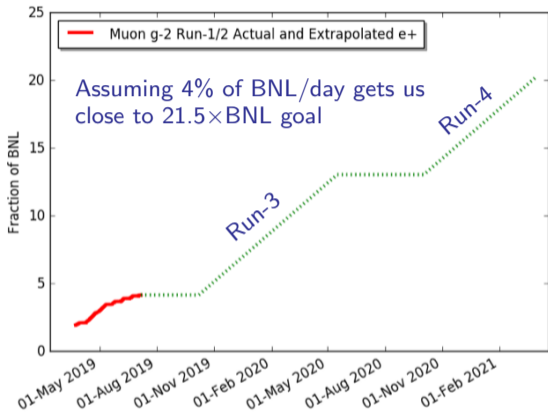
Present status of the experiment:

- ▶ Finished Run-1 and Run-2; analyzing data!
- ▶ After DQC we expect:
 - $\sim 1.4 \times$ BNL for Run-1,
 - $\sim 1.8 \times$ BNL for Run-2.
- ▶ Currently ending shutdown & preparing for Run-3.
- ▶ Goal: publish results of Run-1 by end of 2019.



Current status and plans

- ▶ FNAL E989 is on track to improve the BNL E821 a_μ precision 4-fold:
from 0.54 to ~ 0.14 ppm.
- ▶ Run-3 starts 3-Oct-19, ends 15-May-20.
- ▶ Run-4 will share beam with Mu2e commissioning: 6 months for Muon $g - 2$, 3 months for Mu2e.
- ▶ Goal to publish Run-1 result by end of 2019:



Different approach: reaccelerated low-emittance muon beam and MRI-type storage ring

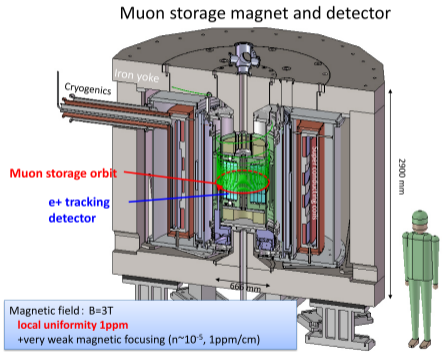
Fermilab E989 $p = 3.1 \text{ GeV}/c$ J-PARC sets $E \equiv 0$.

$$\vec{\omega} = -\frac{e}{m} \left[a_\mu \vec{B} - \left(a_\mu - \frac{1}{\gamma^2 - 1} \right) \frac{\vec{\beta} \times \vec{E}}{c} + \frac{\eta}{2} \left(\vec{\beta} \times \vec{B} - \frac{\vec{E}}{c} \right) \right]$$

$(g - 2)_\mu$
 μEDM

Status and plans:

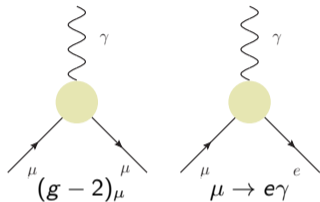
- 2019 continuing R&D; funding request;
- 2020-23 construction;
- 2023 commissioning;
- 2024-26 data run.



Goal uncertainties: similar to Fermilab E989, but **very different systematics** and likely **higher sensitivity to muon EDM**.

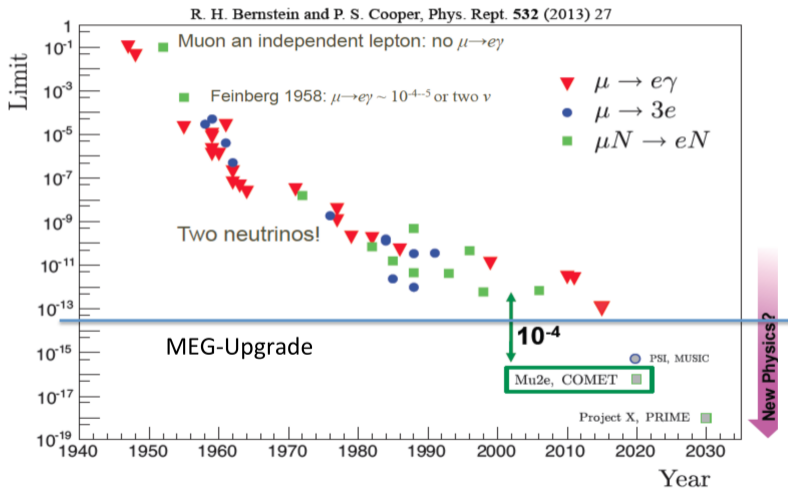
Muon $g - 2$ in relation to CLFV

CLFV processes are highly suppressed in the SM. Muon $g - 2$ and LFV processes share some of the same physics:



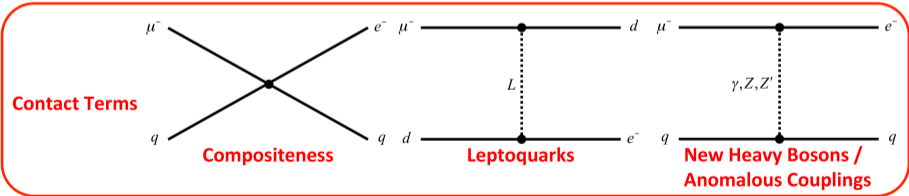
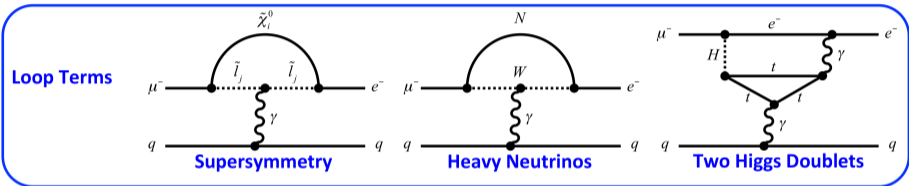
Current and planned experiments:

- ▶ **MEG** and **MEG II** at PSI:
 $\mu \rightarrow e\gamma$ search;
- ▶ **Mu2e** at Fermilab and **COMET** at J-PARC:
 μ to e conversion search;
- ▶ **Mu3e** at PSI:
 $\mu^+ \rightarrow e^+e^-e^+$ search.



Examples of CLFV BSM processes for $\mu^- N \rightarrow e^- N$

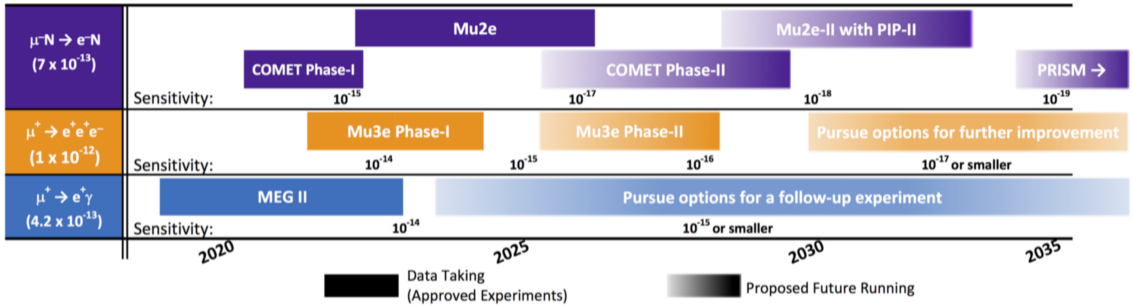
$$L_{CLFV}^{[1]} = \underbrace{\frac{m_\mu}{(\kappa+1)\Lambda^2} \bar{\mu}_R \sigma_{\mu\nu} e_L F^{\mu\nu} + \text{h.c.}}_{\text{Loop Terms}} + \underbrace{\frac{\kappa}{(1+\kappa)\Lambda^2} \bar{\mu}_L \gamma_\mu e_L (\bar{u}_L \gamma^\mu u_L + \bar{d}_L \gamma^\mu d_L) + \text{h.c.}}_{\text{Contact Terms}}$$



[1] A. de Gouvea and P. Vogel, Prog. Part. Nucl. Phys. **71**, 75 (2013). doi:10.1016/j.pnpnp.2013.03.006 [arXiv:1303.4097 [hep-ph]]

κ ... relative coupling strength; Λ ... effective mass scale.

Searches for Charged-Lepton Flavor Violation in Experiments using Intense Muon Beams

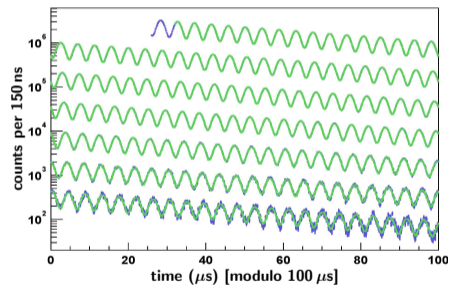


Extra slides



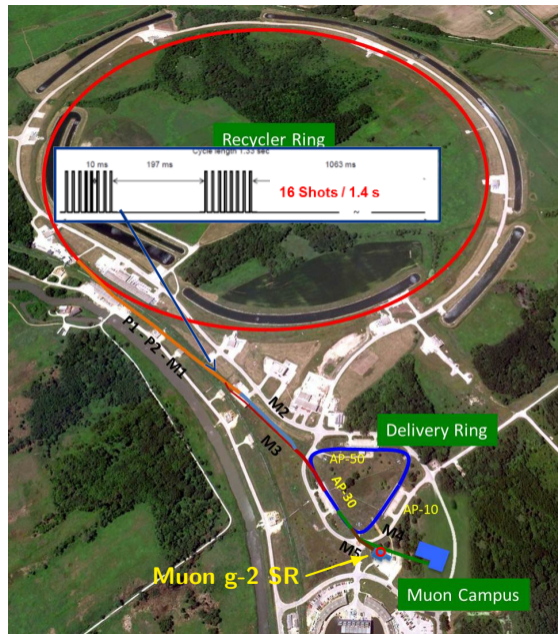
Key points of the experimental method

1. Large quantity of highly polarized muons stored in storage ring:
97% polarized \Rightarrow forward decays,
2. Muon spin precession in magnetic field, ω_a is determined by $g_\mu - 2$,
3. Magic momentum: $p_\mu = 3.09 \text{ GeV}/c$
No effect of \vec{E} on precession when $\gamma_\mu = 29.3$,
4. EW chiral symmetry breaking (PV) gives lab access to average muon spin direction
Number of high energy positrons modulated by ω_a (wiggle plot):
5. To interpret ω_a in terms of g_μ , an independent precise measurement of muon beam averaged $\langle B \rangle$ is critical.



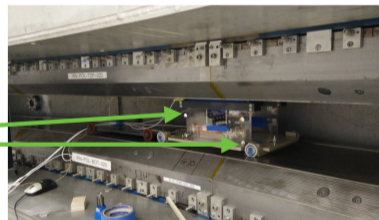
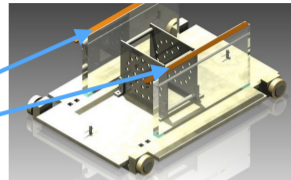
The accelerator complex:

- ▶ 8 GeV p batch into Recycler,
- ▶ split into 4 bunches,
- ▶ extract 1 by 1 to strike target,
- ▶ long FODO channel (alternating focusing and defocusing quads) to collect $\pi \rightarrow \mu\nu$,
- ▶ $p/\pi/\mu$ beam enters DR; protons kicked out; π 's decay away,
- ▶ μ enter storage ring.



Shimming cart

- Lattice of 25 NMR probes (field measurements)
- 4 capacitive gap sensors (pole-pole alignment/separation), 70-nm resolution
- 4 corner-cube retroreflectors (position), $\sim 25 \mu\text{m}$ resolution

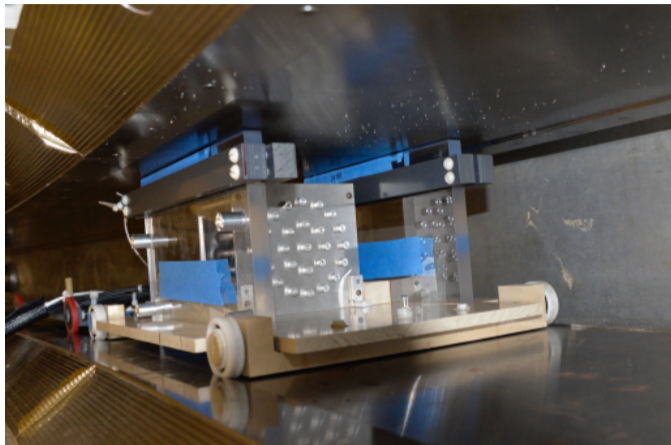


Laser tracker

- Cart position (r, φ, z)

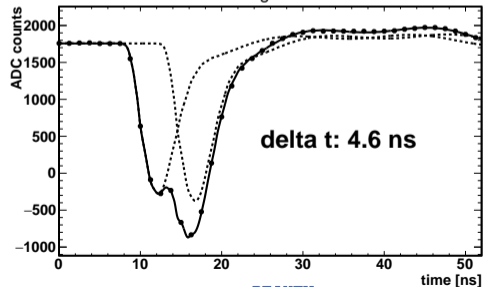
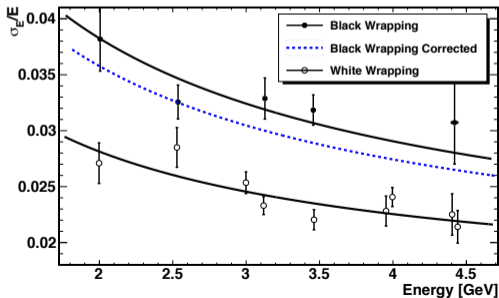
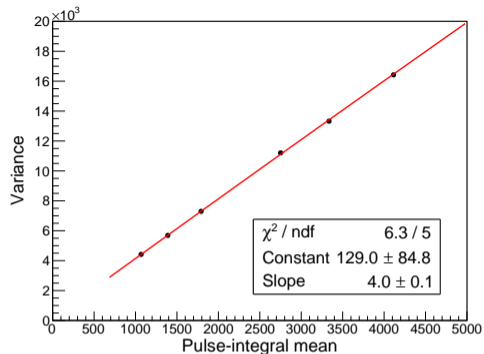
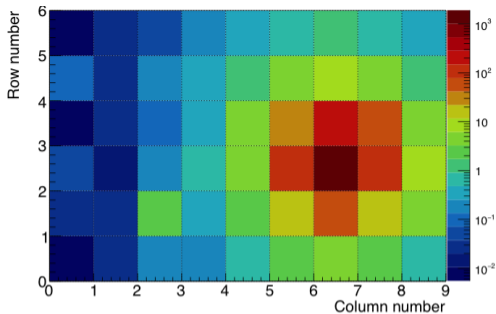


- ▶ Map B at regular intervals (about every two days), with **NMR probe trolley**: 17 proton NMR probes,
 - ▶ monitor B during DAQ with 378 pNMR **fixed probes** in 72 stations;
 - ▶ pulsed pNMR measure B with < 10 ppb single shot precision.
-
- ▶ BNL E821 result:
 - ▶ 1 ppm (azimuth average)
 - ▶ 100 ppm (local variations)



- ▶ FNAL E989 goal:
 - ▶ 1 ppm (azimuth average)
 - ▶ 50 ppm (local variations)

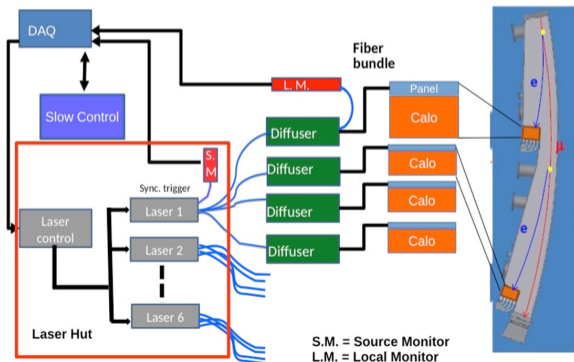
Calorimeter performance



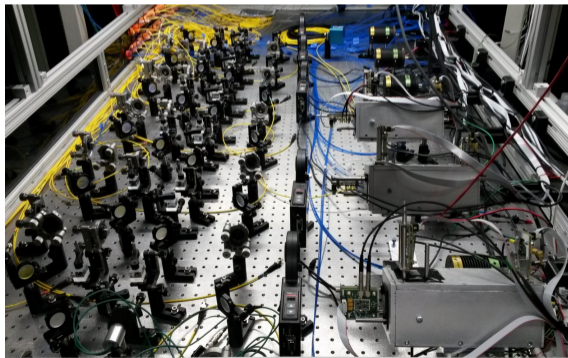
Laser calibration system

Sends trains of laser pulses of known intensity synchronously on all calo. channels; provides:

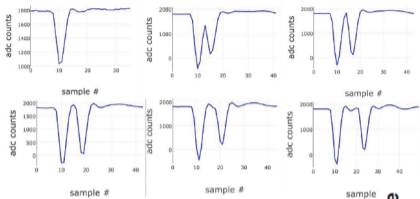
- ▶ absolute calibration of the SiPMs response,
- ▶ short and long term calibration of the of the SiPM gain function,
- ▶ debugging of Calo and DAQ systems,
- ▶ additional synchronization signals.



S.M. = Source Monitor
L.M. = Local Monitor

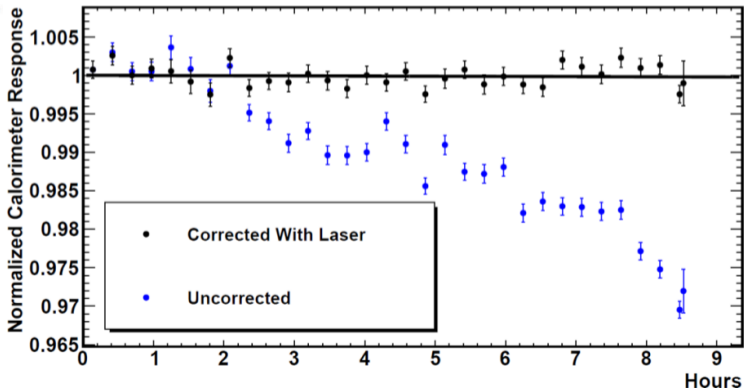


Laser calibration system performance



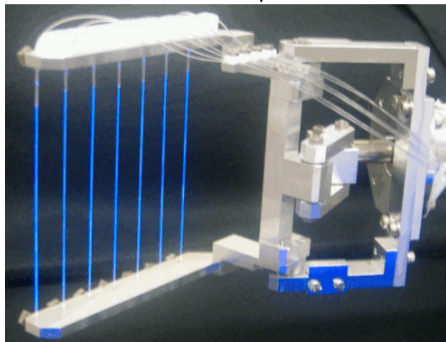
← tuneable individual pulses, tuneable pulse pairs, and “flight simulator” mode.

$10^{-4}/h$ stability demonstrated:



Auxilliary detectors:

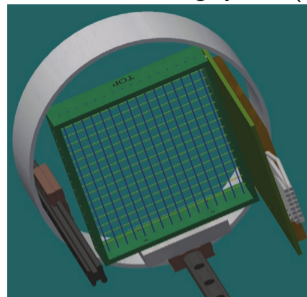
Fiber harps:



2 locations, 2-axis,

- ▶ monitor the muon beam entrance position and angle during commissioning,
- ▶ periodically measure betatron oscillations during data taking runs.

Inflector beam monitoring system (IBMS):



2 det's with 2 planes/each (scint-iber), upstream of inflector; 1 vertical plane (x) downstream of inflector (retracted during data taking):

- ▶ primary diagnostic tool to develop & verify beam optics tune at injection,
- ▶ give relative intensity of each fill,
- ▶ timing of the fill (resolution \ll 150 ns, cyclotron period)

Data acquisition system

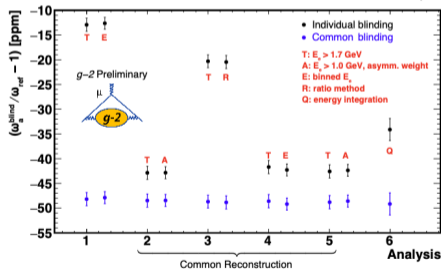
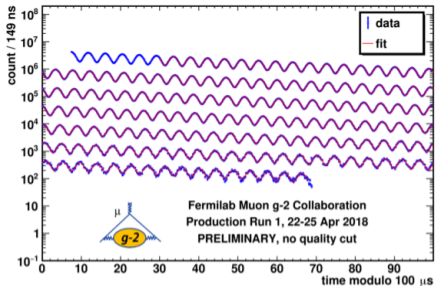
- ▶ Calorimeters, trackers and the laser monitoring system are read out by custom 800 MSPS waveform digitizers.
- ▶ The DAQ produces a deadtime-free record of each $700 \mu\text{s}$ muon fill. We get 12 fills per second, for a total data rate of 20 GB/s.
- ▶ Data from each calorimeter processed by an NVidia Tesla K40 GPU, which processes 33M threads per event.
- ▶ Data are sorted by T-method (chopped islands) and Q-method (current integrated) data, from which timing info can be extracted.
- ▶ The DAQ software is MIDAS based.





Subprojects not discussed here in detail — each presenting great challenges, with a huge effort invested to solve them:

- ▶ Beam transport, optics and optimization through the accelerator complex (enormous and impressive effort by FNAL accelerator group);
- ▶ Inflector magnet optimization (a new one has been built);
- ▶ Kicker system improvements;
- ▶ Electrostatic quadrupole system improvements;
- ▶ Beam dynamics analysis;
- ▶ many more . . .



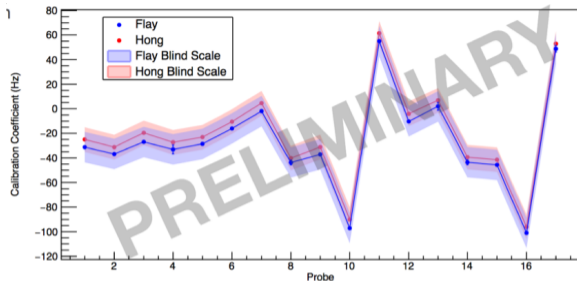
Run-1 ω_a analysis:

- ▶ data are hardware blinded (clock tick frequencies known only to 2 external people);
- ▶ Each analysis has own private software frequency offset.
- ▶ Run-1 has 4 primary data subsets with different Kicker & el-stat Quad settings;
- ▶ 6 groups fitting the frequency with multiple methods;
- ▶ 3 independent event reconstruction efforts;
- ▶ data are corrected for gain & pile-up, binned, and randomized with respect to the cyclotron frequency;
- ▶ full fit functional forms are producing excellent χ^2 and clean residuals.

Sample fit fn.:

$$N(t) = N_0 \Lambda(t) N_{\text{cbo}}(t) N_{\text{vw}} e^{-t/\tau} \{1 + A_0 \cdot A_{\text{cbo}}(t) \cos[\omega_a(R) \cdot t + \phi_0 + \phi_{\text{cbo}}(t)]\}$$

Run-1 $\langle \omega_p \rangle$ (B -field) analysis



- ▶ Fixed probes provide continuous data (outside of muon storage ring volume, SRV) for interpolation between trolley runs.
- ▶ Trolley probe measurements (every ~ 2 days) provide detailed mapping of μ SRV field (multipole expansion).
- ▶ Calibration of trolley probes (TPs) is performed via a special “plunging probe” in the μ SRV, as TPs experience \vec{B} perturbations due to trolley materials, electronics, enclosures.
- ▶ Absolute calibration of plunging probe by two methods:
 - using spherical-shaped H_2O sample (as was done in BNL E821), and
 - using polarized 3He (an independent technique 3 newly implemented in FNAL E989).
- ▶ Two(+) independent blinded analyses; they agree within the blinding bands; a preliminary Run-1 estimate of $\langle B \rangle$ is imminent.

FNAL Muon $g - 2$ experiment final uncertainty goals

ω_a systematic uncertainty summary^[1].

Category	BNL [ppb]	FNAL Goal [ppb]
Gain Changes	120	20
Pileup	80	40
Lost Muons	90	20
CBO	70	< 30
E-field & Pitch Corrections	50	30
Total (Quadrature Sum)	190	70

a_μ uncertainty summary^[1,2].

Category	BNL [ppb]	FNAL Goal [ppb]
Total Statistical Uncertainty	460	100
Total Systematic Uncertainty	280*	100
Total (Quadrature Sum)	540*	140

* The net systematic is across 3 running periods.

[1] J. Grange et al. [Muon $g-2$ Collaboration], arXiv:1501.06858 [physics.ins-det].

[2] M. Tanabashi et al. (PDG), Phys. Rev. D **98** (2018) 030001.

$\langle\omega_p\rangle$ (B-field) systematic uncertainty summary^[1].

Category	BNL [ppb]	FNAL Goal [ppb]
Absolute Field Calibration	50	35
Trolley Probe Calibrations	90	30
Trolley Measurements Of B_0	50	30
Fixed Probe Interpolation	70	30
Muon Distribution	30	10
Time-dependent External Magnetic Fields	-	5
Others (Collective Smaller Effects)	100	30
Total (Quadrature Sum)	170	70

Improvement in uncertainties

E821 Error	Size [ppm]	Plan for the E989 $g - 2$ Experiment	Goal [ppm]
Gain changes	0.12	Better laser calibration; low-energy threshold; temperature stability; segmentation to lower rates; no hadronic flash	0.02
Lost muons	0.09	Running at higher n -value to reduce losses; less scattering due to material at injection; muons reconstructed by calorimeters; tracking simulation	0.02
Pileup	0.08	Low-energy samples recorded; calorimeter segmentation; Cherenkov; improved analysis techniques; straw trackers cross-calibrate pileup efficiency	0.04
CBO	0.07	Higher n -value; straw trackers determine parameters	0.03
E-Field/Pitch	0.06	Straw trackers reconstruct muon distribution; better collimator alignment; tracking simulation; better kick	0.03
Diff. Decay	0.05 ¹	better kicker; tracking simulation; apply correction	0.02
Total	0.20		0.07

E821 Error	Size [ppm]	Plan for the E989 $g - 2$ Experiment	Goal [ppm]
Absolute field calibrations	0.05	Special 1.45 T calibration magnet with thermal enclosure; additional probes; better electronics	0.035
Trolley probe calibrations	0.09	Absolute cal probes that can calibrate off-central probes; better position accuracy by physical stops and/or optical survey; more frequent calibrations	0.03
Trolley measurements of B_0	0.05	Reduced rail irregularities; reduced position uncertainty by factor of 2; stabilized magnet field during measurements; smaller field gradients	0.03
Fixed probe interpolation	0.07	More frequent trolley runs; more fixed probes; better temperature stability of the magnet	0.03
Muon distribution	0.03	Additional probes at larger radii; improved field uniformity; improved muon tracking	0.01
Time-dependent external B fields	–	Direct measurement of external fields; simulations of impact; active feedback	0.005
Others	0.10	Improved trolley power supply; trolley probes extended to larger radii; reduced temperature effects on trolley; measure kicker field transients	0.05
Total	0.17		0.07

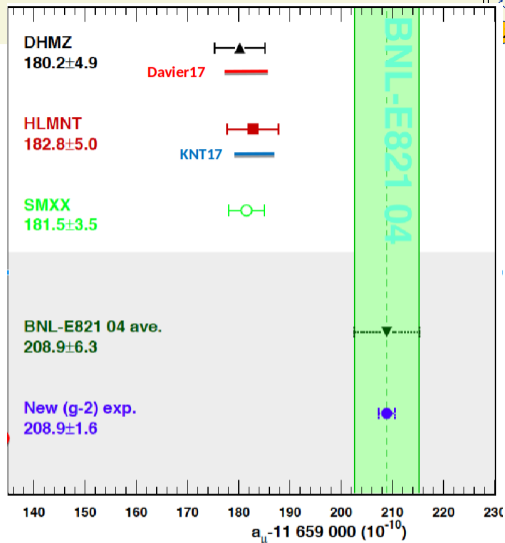
Ultimate goal of E989

From 2013 Snowmass white paper:
(values given in units of 10^{-11})

Uncertainty	Dav11	Hag11	Future
$\delta a_{\mu}^{\text{SM}}$	49	50	35
$\delta a_{\mu}^{\text{HLO}}$	42	43	26
$\delta a_{\mu}^{\text{HLbL}}$	26	26	25
$\delta(a_{\mu}^{\text{EXP}} - a_{\mu}^{\text{SM}})$	80	80	40

2017 updates:

Uncertainty	DHMZ17	KNT17	Future
$\delta a_{\mu}^{\text{SM}}$	42	37	35
$\delta a_{\mu}^{\text{HLO}}$	33	26	26
$\delta a_{\mu}^{\text{HLbL}}$	26	26	25
$\delta(a_{\mu}^{\text{EXP}} - a_{\mu}^{\text{SM}})$	76	73	40

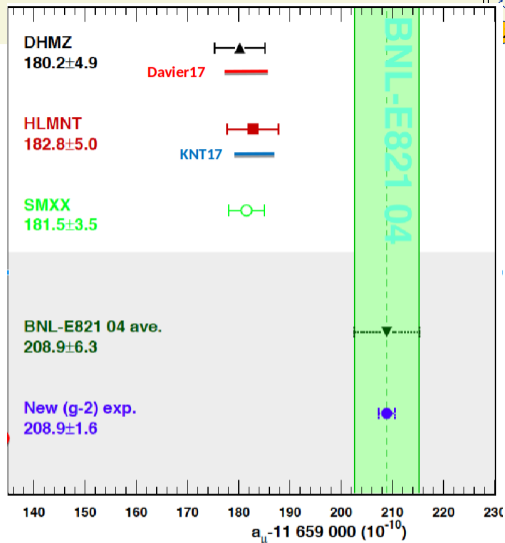


From 2013 Snowmass white paper:
(values given in units of 10^{-11})

Uncertainty	Dav11	Hag11	Future
$\delta a_{\mu}^{\text{SM}}$	49	50	35
$\delta a_{\mu}^{\text{HLO}}$	42	43	26
$\delta a_{\mu}^{\text{HLbL}}$	26	26	25
$\delta(a_{\mu}^{\text{EXP}} - a_{\mu}^{\text{SM}})$	80	80	40

2017 updates:

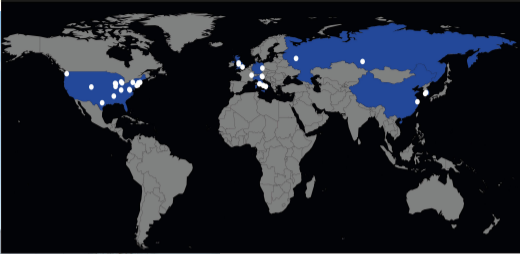
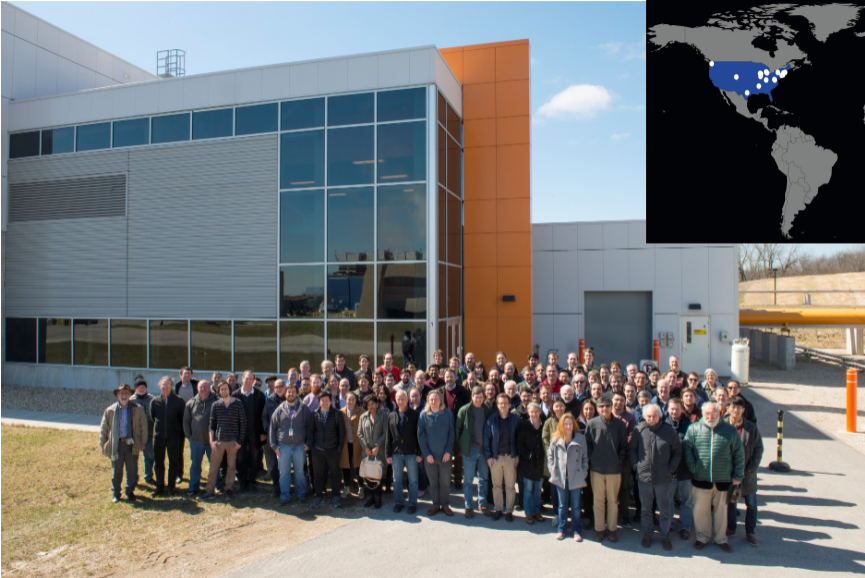
Uncertainty	DHMZ17	KNT17	Future
$\delta a_{\mu}^{\text{SM}}$	42	37	35
$\delta a_{\mu}^{\text{HLO}}$	33	26	26
$\delta a_{\mu}^{\text{HLbL}}$	26	26	25
$\delta(a_{\mu}^{\text{EXP}} - a_{\mu}^{\text{SM}})$	76	73	40



For the same SM and EXP central values, the discrepancy would increase from $\sim 3.5\sigma$ to $\sim 7\sigma$.

The big SR magnet move (2013)







USA

- Boston
- Cornell
- Illinois
- James Madison
- Kentucky
- Massachusetts
- Michigan
- Michigan State
- Mississippi
- North Central
- Northern Illinois
- Regis
- Virginia
- Washington

USA National Labs

- Argonne
- Brookhaven
- Fermilab



China

- Shanghai Jiao Tong



Germany

- Dresden



Italy

- Frascati
- Molise
- Naples
- Pisa
- Roma Tor Vergata
- Trieste
- Udine



Korea

- CAPP/ISB
- KAIST



Russia

- Budker/Novosibirsk
- JINR Dubna



United Kingdom

- Lancaster/Cockcroft
- Liverpool
- Manchester
- University College London

